

## Article

# An Assessment of the Possibility of Restoration and Protection of Territories Disturbed by Thermokarst in Central Yakutia, Eastern Siberia

Aleksandr Zhirkov <sup>1,\*</sup>, Maksim Sivtsev <sup>1</sup>, Vasylii Lytkin <sup>1,2</sup>, Anatolii Kirillin <sup>1</sup>, Antoine Séjourné <sup>3</sup>  
and Zhi Wen <sup>4</sup>

<sup>1</sup> Melnikov Permafrost Institute, Siberian Branch of the Russian Academy of Sciences, Yakutsk 677010, Russia

<sup>2</sup> The Institute for Humanities Research and Indigenous Studies of the North, Siberian Branch of the Russian Academy of Sciences, Yakutsk 677000, Russia

<sup>3</sup> University Paris-Saclay, Gif-sur-Yvette, 91190 Paris, France

<sup>4</sup> State Key Laboratory of Frozen Soil Engineering, Northwest Institute of Eco-Environment and Resources, Chinese Academy of Sciences, Lanzhou 730000, China

\* Correspondence: zhirkov\_af@mail.ru

**Abstract:** Rapid permafrost degradation is observed in northern regions as a result of climate change and expanding economic development. Associated increases in active layer depth lead to thermokarst development, resulting in irregular surface topography. In Central Yakutia, significant areas of the land surface have been deteriorated by thermokarst; however, no mitigation or land rehabilitation efforts are undertaken. This paper presents the results of numerical modeling of the thermal response of permafrost to changes in the active layer hydrothermal regime using field data from the village of Amga, Republic of Sakha (Yakutia), and mathematical analysis. The results suggest that restoring a thick ice-enriched layer will require increasing the pre-winter soil moisture contents in order to increase the effective heat capacity of the active layer. Snow removal or compaction during the winter is recommended to maximize permafrost cooling. The thickness of the restored transition layer varies from 0.3 to 1.3 m depending on soil moisture contents in the active layer. The modeling results demonstrate that damaged lands can be restored through a set of measures to lower the subsurface temperatures. A combination of the insulating layer (forest vegetation) and the high heat capacity layer (transition layer) in the atmosphere–ground system would be more effective in providing stable geocryological conditions.

**Keywords:** permafrost; ice-rich sediments; thermokarst; yedoma (ice complex); active layer; transition layer; permafrost degradation; transition layer restoration



**Citation:** Zhirkov, A.; Sivtsev, M.; Lytkin, V.; Kirillin, A.; Séjourné, A.; Wen, Z. An Assessment of the Possibility of Restoration and Protection of Territories Disturbed by Thermokarst in Central Yakutia, Eastern Siberia. *Land* **2023**, *12*, 197. <https://doi.org/10.3390/land12010197>

Academic Editors: Yoshihiro Iijima and Le Yu

Received: 27 October 2022

Revised: 25 December 2022

Accepted: 30 December 2022

Published: 7 January 2023



**Copyright:** © 2023 by the authors. Licensee MDPI, Basel, Switzerland. This article is an open access article distributed under the terms and conditions of the Creative Commons Attribution (CC BY) license (<https://creativecommons.org/licenses/by/4.0/>).

## 1. Introduction

The observed increase in air temperature in the Arctic and Subarctic regions is greater than the global mean temperature increase, with associated rapid transformations of the environment, including the thaw of permafrost [1]. The frequency and magnitude of landscape disturbance related to permafrost degradation are increasing [2–4]. The thawing of permafrost poses significant risks associated with enhanced greenhouse effects (greenhouse gas emission), damage to infrastructure, and harm to subsistence livelihoods. Understanding the processes and mechanisms of permafrost degradation in response to ongoing climate change is critical in projecting future environmental changes in the Arctic and Subarctic.

Permafrost degradation is of particular concern in areas of ice-rich Yedoma deposits which are most vulnerable to thermokarst processes. Thermokarst can substantially modify natural and anthropogenic landscapes, creating difficulties for development activities. The consequences of permafrost thawing are already becoming apparent, with damage to

buildings, linear infrastructure, homesteads, and farmlands, causing dramatic ecological and socioeconomic impacts. As the Republic of Sakha (Yakutia) Governor reported at the Northern Sustainable Development Forum on Climate Change and Permafrost in September 2021, the arable land area in the region has been reduced by 57%, from 107,000 ha in 1990 to 46,000 ha in 2016, due to the degradation of permafrost [5–9].

Thermokarst processes are most active in the open, natural, or anthropogenic landscapes where the transition layer is very thin (0–0.2 m) [10,11], while in the areas covered by boreal forests, this zone may be as thick as 0.7–1.0 m [11,12]. Following Efimov and Grave [12], Shur [13], and Yanovsky [14], we understand the transition layer as an ice-rich layer between the active layer and the top of permafrost (usually wedge ice), which acts as a buffer and protects permafrost from deep thawing on account of the latent heat required for phase transitions. Destruction of this protective layer due to climate warming can lead to rapid thermokarst development [12,15]. In this context, research is needed to assess transition layer restoration as a potential land rehabilitation method in ice-rich permafrost areas.

One of the main parameters affecting the dynamics of the active layer is atmospheric precipitation, both solid in the form of snow and liquid in the form of rain [16–20]. Thus, an increase in the thickness of the snow cover to the depth of the active layer has a negative effect. With its increase, the freezing of the active layer slows down and the accumulation of negative temperatures in permafrost soils decrease due to thermal protection from the winter cold, which leads to an increase in the depth of the active layer in subsequent years [16,17]. An increase in liquid atmospheric precipitation also leads to an increase in the depth of the active layer. Such processes were observed in Alaska, where the depth of the active layer increased by  $0.7 \pm 0.1$  cm for each cm of summer precipitation exceeding the average annual norms, and in the Kolyma Lowland (Siberian tundra), the depth of the active layer increased by 35% when there was a 120% increase in the amount of rainfall compared to the average annual amount of precipitation [18–20].

However, reverse processes were also observed, associated with a decrease in the depth of the active layer with an increase in the amount of summer precipitation in Central Yakutia. Extensive investigations of the hydrothermal regime of the active layer have been conducted by P.P. Gavriliev's group at the Melnikov Permafrost Institute since the 1970s in natural and agricultural lands (alasses and river valleys) [21–23]. These studies provided insights into the seasonal moisture and temperature dynamics of the active layer, as well as surface degradation due to the warming and cooling effects of land reclamation and agricultural practices e.g., [24–28]. They also led to the first attempts to remedy the cultivated fields damaged by thermokarst [29–31]. One such rehabilitation project involved grading and filling of thaw pits, 0.2 to 0.7 m deep, in a 70 ha field. As a result of these measures, the protective layer above the ice wedges attained a thickness equal to the depth of the pits, and the field was brought back into use. Several years later, however, a repeated increase in thaw depth re-initiated thermokarst, causing the field to be abandoned. The same processes were noted in the mountain permafrost of the Qinghai-Tibet Plateau [32,33].

Several investigations have examined the effects of rainfall infiltration amounts on the temperature regime of soils and demonstrated experimentally that a significant, long-term (over 3 years) increase in rainfall amounts can locally lower the permafrost temperatures [34–36]. This was shown to result from the increased ice contents due to water saturation, changes in soil thermal properties, and latent heat effects.

Based on the findings from previous land reclamation and remediation studies, we hypothesize that lands deteriorated by thermokarst may be effectively restored by planning, moistening, and snow removal. The basic aspect of research is directed toward characterizing the parameters controlling thermokarst initiation and development, as well as finding effective ways to quickly restore and maintain the protective transition layer in natural landscapes. In practical terms, the results of the research will be used as the basis for the implementation of restoration and maintenance programs for agricultural and built

environments. In this paper, we present theoretical justification for the hypothesis using mathematical modeling.

## 2. Materials and Methods

### 2.1. Study Area

The study area is located on the north side of the Amga River in southeastern Central Yakutia (Figure 1). Geomorphologically, it is part of the Pre-Lena Plateau and represents a fluvial terrace above the floodplain, with elevations ranging between 217 and 243 m. It is composed of silty sediments which contain large ice wedges, which reach 15–20 m in vertical extent. The area has a strong continental climate. The mean annual air temperature at the Amga weather station is  $-8.3\text{ }^{\circ}\text{C}$ , with mean January and July temperatures of  $-40.8\text{ }^{\circ}\text{C}$  and  $+17.6\text{ }^{\circ}\text{C}$ , respectively. The mean annual precipitation is 270 mm [37].

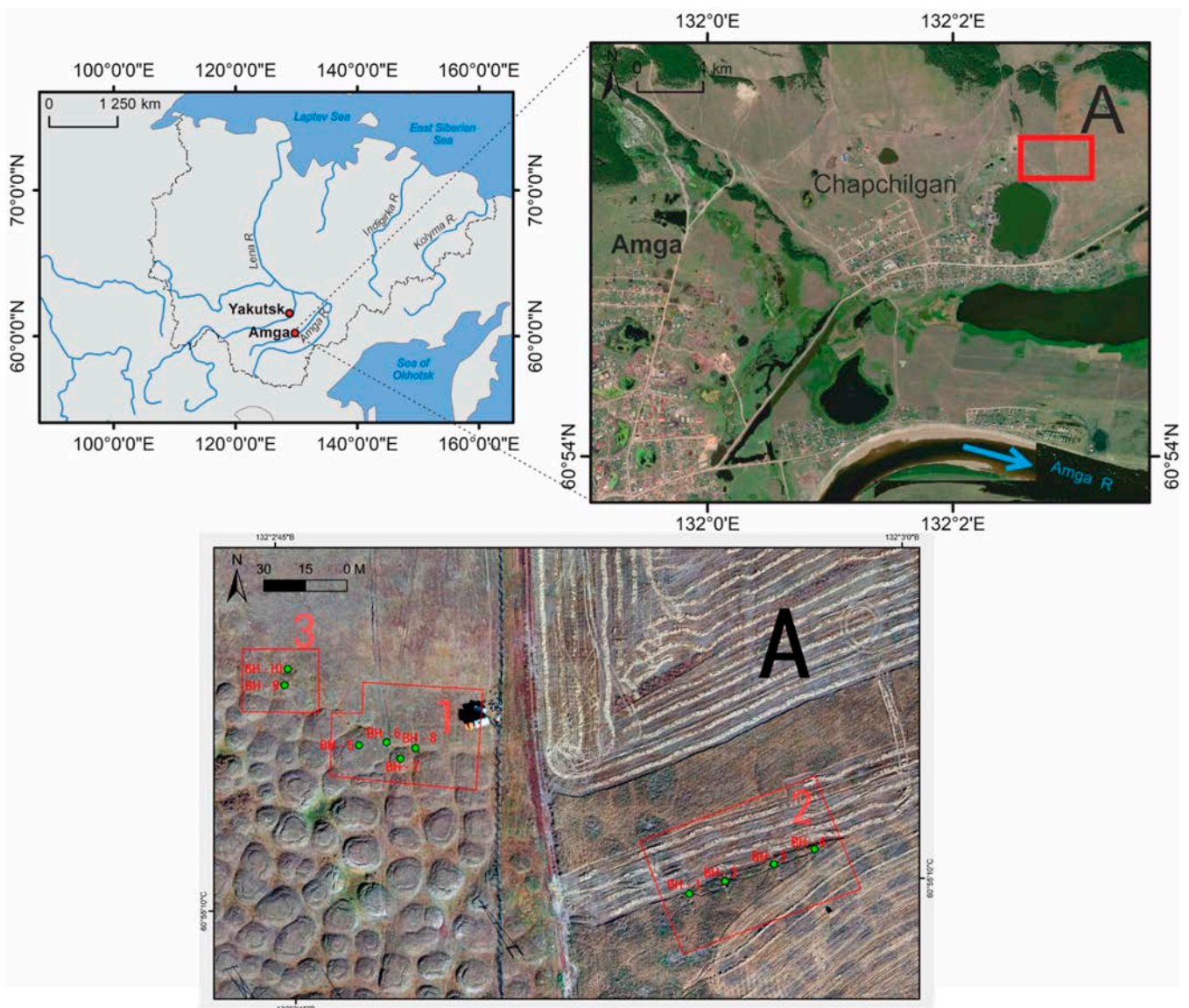


**Figure 1.** Location of the study area. 1—experimental area №1, 2—experimental area №2, and 3—control area.

According to the Permafrost Landscape Map of Yakutia, the study area lies within the Amga–Aldan Middle Taiga Province with gently rolling topography and continuous permafrost [38]. The terrain unit is classified as colluvial–soliflual sloping terrain with

ground temperatures in the range of  $-1.5\text{ }^{\circ}\text{C}$  to  $-1\text{ }^{\circ}\text{C}$  and permafrost thickness in the range of 200–300 m. The active layer thickness in the study area varies from 2.2 to 2.8 m.

Thermokarst processes are observed within and adjacent to the study area, resulting in surface subsidence and subsequent development of thermokarst ponds (Figure 2). Because the ice wedges occur close to the surface (at 2.2 to 2.8 m deep), deterioration of the permafrost terrain is significant.



**Figure 2.** Thermokarst microrelief formed as a result of the thermokarst processes (permafrost degradation) in the study area.

## 2.2. Thermokarst Remediation Procedure

The proposed procedure for land remediation by restoring the protective layer in Yedomo deposits involves the following set of measures:

Stage I: late summer—grading with machinery to level off the thermokarst topography. This stage is not considered in the present study.

Stage II: autumn (before freezing air temperatures)—irrigation to increase volumetric soil moisture contents in the active layer to full saturation (45 to 70% for clay silts and sandy silts, respectively). Before irrigation, the optimal amount of water to be applied should be determined based on site-specific soil moisture regimes.

Stage III: winter—snow removal or snow compaction to provide deeper freezing of the moist soils.

These steps would lead to the restoration of the protective layer, provided that adequate moisture levels are employed.

Stage IV: spring—revegetation to maintain the restored protective layer, i.e., resumption of sowing activities in agricultural lands or the creation of forest stands by planting trees in natural landscapes. In this modeling study, the revegetation stage is considered in all variants and scenarios as shading.

If fully implemented, these measures are expected to lead to the rehabilitation of the lands damaged by thermokarst (Figure 3).

Based on the proposed measures, a mathematical heat and mass transfer model has been developed to determine the conditions optimal for the restoration of the protective layer.

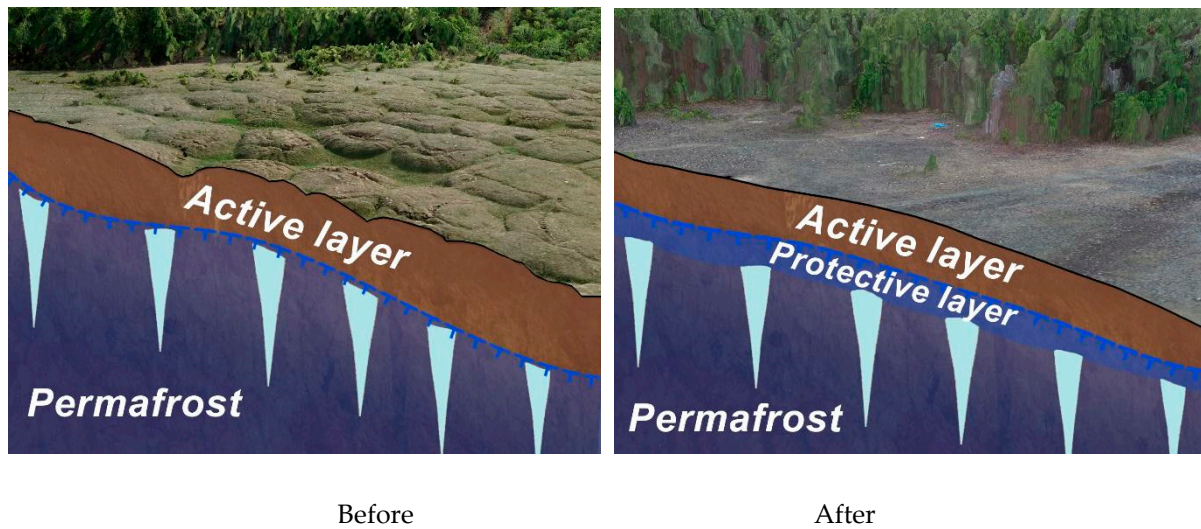


**Figure 3.** Schematic of thermokarst remediation by restoring the transition layer.

### 2.3. Mathematical Modeling

We used the Frost 3D Universal software package to simulate optimal conditions for restoring the protective transition layer.

Frost 3D Universal [39] is a software suite for modeling heat and mass transfer in permafrost considering external thermal impacts. It allows one to develop scientific models of permafrost thermal regimes under the thermal influence of engineering structures, as well as of climate change.

The solution to the three-dimensional unsteady heat transfer problem [40] in Frost 3D Universal is based on the well-proven heat conduction Equation (1), which takes into account phase change and convective heat transport:

$$\left( C(T) + \rho_b L \cdot \frac{\partial w_w(T)}{\partial T} \right) \frac{\partial T}{\partial t} + \nabla(-\lambda(T)\nabla T) + C_w u \nabla T = 0 \quad (1)$$

where  $T$  is the temperature, °C;  $C(T)$  is the volumetric heat capacity of soil as a function of temperature, J/(m<sup>3</sup>·°C);  $w_w(T)$  is the unfrozen water content (decimal) as a function of temperature;  $\rho$  is the soil density, kg/m<sup>3</sup>;  $L$  is the latent heat, J/kg;  $t$  is the time, s;  $\lambda(T)$  is the thermal conductivity of soil as a function of temperature, W/(m·°C);  $C_w$  is the volumetric heat capacity of water, J/(m<sup>3</sup>·°C); and  $u$  is the soil water flow velocity vector, m/s.

In the software suite, the temperature volumetric dependence of heat capacity and thermal conductivity is calculated in accordance with the following Expressions (2) and (3):

$$C(T) = C_f \left( 1 - \frac{w_w(T)}{w_{tot}} \right) + C_{th} \left( \frac{w_w(T)}{w_{tot}} \right) \quad (2)$$

$$\lambda(T) = \lambda_f \left( 1 - \frac{w_w(T)}{w_{tot}} \right) + \lambda_{th} \left( \frac{w_w(T)}{w_{tot}} \right) \quad (3)$$

where  $C_{th}$  and  $C_f$  are the volumetric heat capacity of soil in a thawed and frozen state, J/(m<sup>3</sup>·°C);  $\lambda_{th}$  and  $\lambda_f$  are the thermal conductivity of soil in a thawed and frozen state, W/(m·°C);  $w_{tot}$  is the total weight of soil moisture, (decimal); and  $w_w(T)$  is the dependence of the amount of unfrozen water in the soil on temperature, (decimal). In the heat and mass transfer model, the phase change upon freezing and thawing was assumed to be localized at the phase boundary (at a single temperature). This assumption was made because, in this particular case, the soil had a background (normal) unfrozen water content and, hence, calculating the freezing and thawing process over a temperature range was not warranted.

Appropriate physical and thermal properties were specified for all soil types and materials present in the model domain. Additionally, boundary conditions were specified

for all heat transfer conditions used in the model. The upper boundary condition was represented by the third-type boundary condition (Newton's law) (4), which requires specifying the temperature, heat transfer coefficient and, if necessary, additional heat flux as a function of time:

$$n \cdot (\lambda \nabla T) = \alpha(t) \cdot (T_{ext}(t) - T) + q_0(t) \quad (4)$$

where  $\alpha$  is the heat transfer coefficient,  $W/(m^2 \cdot ^\circ C)$ ;  $T_{ext}$  is the exterior temperature,  $^\circ C$ ;  $T$  is the ground temperature,  $^\circ C$ ;  $q_0$  is the heat flux,  $W/m^2$ ; and  $t$  is the time, s.

The heat transfer coefficient ( $\alpha$ ) between the soil surface and the atmosphere as a function of wind speed was calculated using the Kurtner–Chudnovsky equation [41].

Soil water flow is modeled in Frost 3D Universal based on the widely used Equation (5), derived from Darcy's law [42]:

$$\nabla \cdot (-K \nabla H) = 0 \quad (5)$$

From this, the water flow velocity vector is determined by Equation (6):

$$u = -K \nabla H \quad (6)$$

where  $H$  is the hydraulic head, m;  $K$  is the hydraulic conductivity, m/s; and  $u$  is the water flow velocity vector.

For a hydrological boundary condition, the following is available:

The hydraulic head is calculated using Equation (7):

$$H = H_{ext}(t) \quad (7)$$

where  $H_{ext}$  is the external flow rate, m/s.

The three-dimensional conduction equation is solved numerically using the explicit finite difference technique [43]. The finite difference technique is a grid method, i.e., the problem's domain is discretized into a hexahedral grid and calculations are made at nodes of the grid system, with a finite difference equation formulated for each node in accordance with the difference scheme stencil used. A system of linear equations is generated. By solving the equation system, the relevant information in the region of interest is obtained.

#### 2.4. Input Data

To calculate the ground temperature regimes, a model domain,  $16 \times 24$  m in size along the X and Y axes and the dimensions of one grid cell are 0.05 cm (Figure 4), was defined based on drilling data.

The mean monthly air temperatures and heat transfer coefficients in Amga for the last 10 years were applied as external parameters (Table 1) [44]. These were chosen because the Roshydromet mean monthly temperatures (calculated normals from 1966) [45] are lower and do not consider climate change over the past 30 years.

The initial ground temperature distribution is given in Table 2. The simulation period starts in September 2021.

As the geothermal heat flux was assumed to have no effect on the ground temperature profile, a constant permafrost temperature at the depth of zero annual amplitude [46,47] was set at the lower boundary of the model, equal to  $-1.5$   $^\circ C$ .

For open terrain, the third-type boundary conditions were used:

- air temperature (Table 1);
- heat transfer coefficient (Table 1) calculated from wind speed;
- snow depth (Table 3) [44].

Snow depth was set using data from the Amga meteorological station for the past 12 years [44]. Snow thermal conductivity was estimated using Proskuryakov's equation [39].

The physical and thermal properties of the materials were obtained by us in the laboratory MPI SB RAS and are presented in Tables 4 and 5.

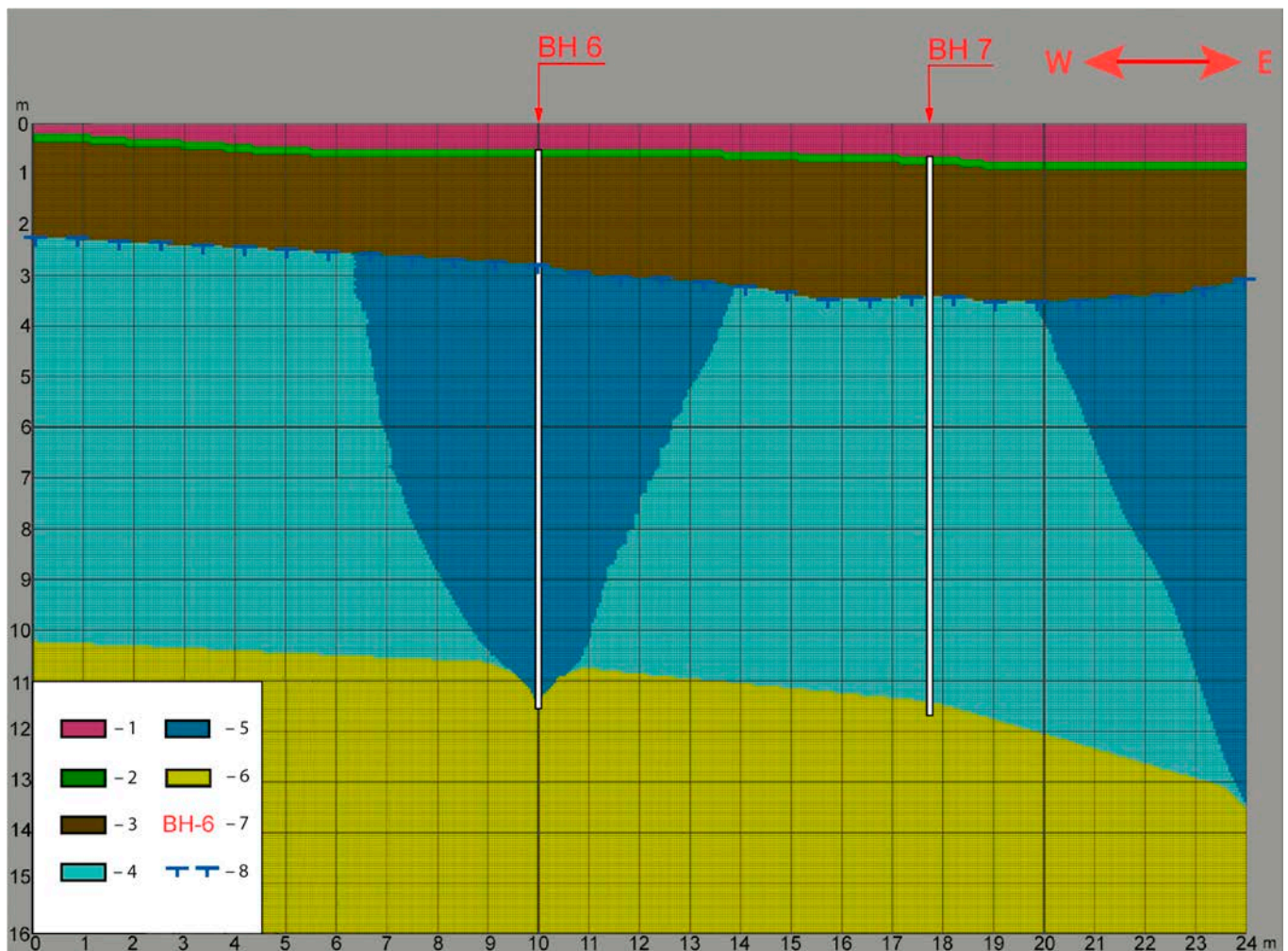


**Figure 4.** Computational domain. Legend: 1—atmosphere, 2—organic cover, 3—clayey silt, 4—sandy silt, 5—wedge ice, 6—sand, 7—borehole and its ID, and 8—top of permafrost.

**Table 1.** Mean monthly values of air temperature and heat transfer coefficients.

Date	Temperature, °C	Heat Transfer Coefficient, W/m <sup>2</sup> ·K
January	−38.36	8.2969
February	−34.82	8.6321
March	−19.82	11.8165
April	−3.34	16.0065
May	8.68	17.8082
June	16.19	15.9646
July	18.96	14.8333
August	15.16	14.0791
September	5.97	14.8333
October	−7.36	14.1629
November	−27.21	10.3919
December	−38.39	8.6321

**Table 2.** Ground temperature distribution.

Depth, m	Temperature, °C
0	16.34
0.2	15.73
0.4	15.07
0.6	13.89
0.8	12.29
1	10.54
1.2	8.7
1.4	6.94
1.6	5.33
1.8	3.73
2	2.22
2.2	0.97
2.5	−0.16
3	−0.39
3.5	−0.5
4	−0.6
4.5	−0.62
5	−0.69
7.5	−0.93
10	−1.1

**Table 3.** Snow depth (m) average over the last 12 years at Amga meteorological station.

Month											
I	II	III	IV	V	VI	VII	VIII	IX	X	XI	XII
0.28	0.33	0.35	0.19	0	0	0	0	0	0.07	0.18	0.24

**Table 4.** Physical properties of materials in the modeling.

Material	$\rho$	Moisture Content		$T_{pc}$
		$W_{tot}$	$W_w$	
Clayey silt	1700	0.4	Similar to that of clayey silt (0.07 < plasticity index < 0.13)	−0.2
Sandy silt	1409	0.54	Similar to that of sandy silt (0.02 < plasticity index < 0.07)	−0.16
Wedge ice	900	1.14	Similar to that of ice	0
Sand	1800	0.2	Similar to that of sand (plasticity index < 0.02)	−0.1
Organic layer	1470	0.19	Similar to that of sandy silt (0.02 < plasticity index < 0.07)	−0.65
Ice with $\leq 20\%$ soil	1470	0.598	Similar to that of ice	0.49

$\rho$ —density, kg/m<sup>3</sup>;  $W_{tot}$ —total gravimetric moisture content (decimal);  $W_w$ —unfrozen water content curve function; and  $T_{pc}$ —phase change temperature, °C.

**Table 5.** Thermal properties of materials in the modeling.

Material	$\lambda$		$C_{\gamma}$	
	Thawed	Frozen	Thawed	Frozen
Clayey silt	1.3	1.8	2,889,000	2,278,000
Sandy silt	1.47	2.4	3,488,000	2,140,000
Wedge ice	-	2.6		1,890,000
Sand	1.9	2.5	1,600,000	1,400,000
Organic mat	1.2	1.8	1,500,000	1,180,000
Ice with $\leq 20\%$ soil	1.77	2.38	1,856,000	1,301,000

$\lambda$ —thermal conductivity, W/(m·K) and  $C_{\gamma}$ —volumetric heat capacity, J/(m<sup>3</sup>·K).

### 3. Results

Three soil moisture variants were investigated to determine optimal conditions for restoring the protective layer (Table 6).

**Table 6.** Three different simulations with soil moisture variants in the modeling.

No.	Variant
1	Soil moisture contents within the active layer in the warm season are taken to equal the saturated moisture contents
2	Soil moisture contents within the active layer are set as average moisture contents over the warm season (natural moisture contents)
3	Soil moisture contents within the active layer are set as warm season average; pre-winter moisture contents are set every 3 years at saturated moisture contents

Snow cover is an important factor controlling the hydrothermal regime of permafrost. For each moisture variant, five scenarios of snow removal and snow compaction were applied (Table 7).

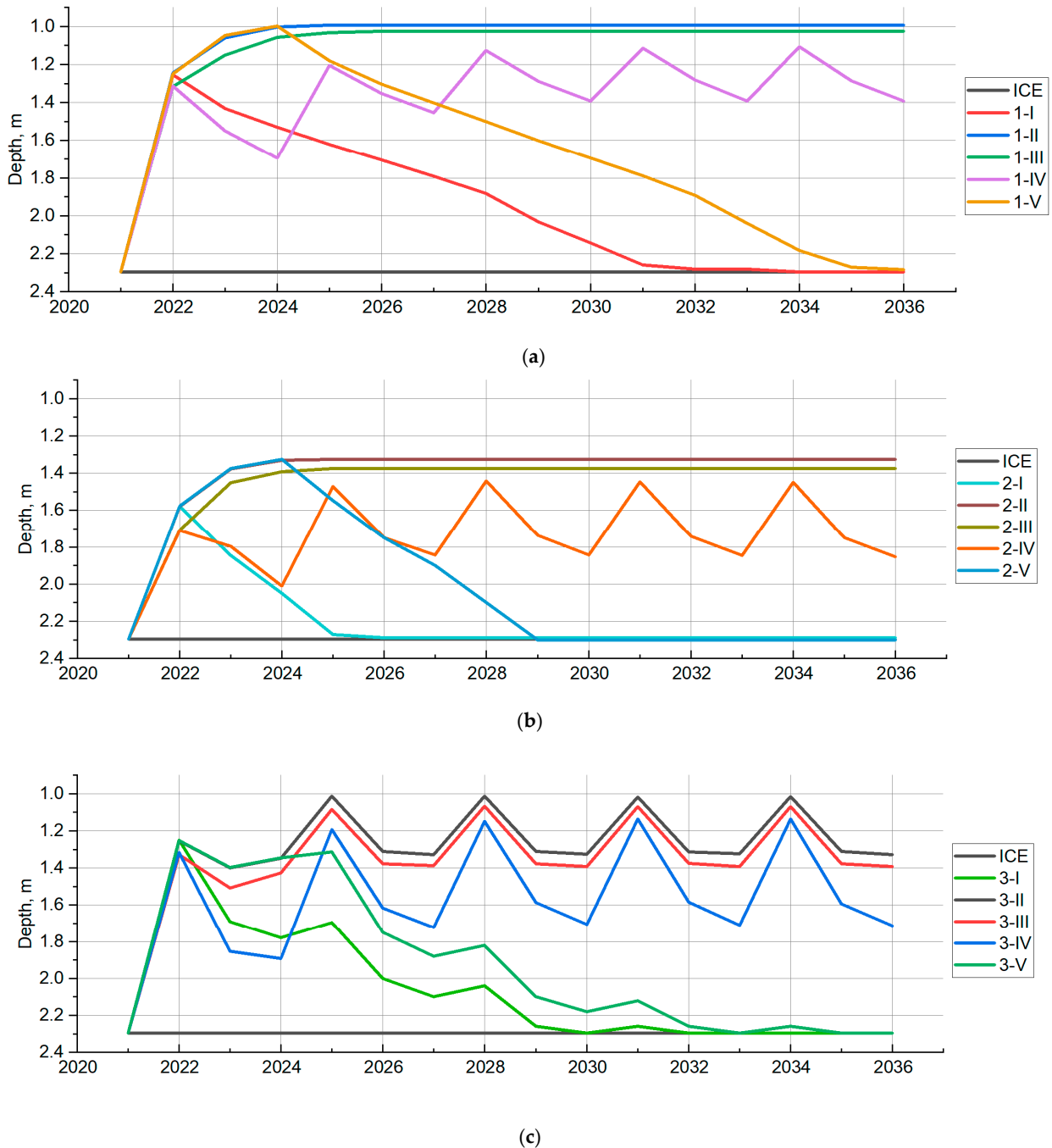
**Table 7.** Snow removal/compaction scenarios in the modeling.

No.	Scenario
I	Snow cover is absent within the first year and equal to the recent 10-year average in subsequent years
II	Snow cover is absent (snow removal) throughout the simulation period
III	Snow cover is dense (snow compaction) throughout the simulation period
IV	Snow compaction every 3 years
V	Snow cover is absent for the first 3 years and equal to the recent 10-year average in subsequent years

In each case, the air temperature was employed with the observed trend. The trend calculated from the mean annual air temperatures since 1966 is 0.05 °C/yr (0.5 °C/decade) for the Amga meteorological station [48,49]. Additionally, vegetation cover in the form of grassland was considered in all scenarios by changing the wind speed so that it did not exceed 1.1 m/s [50].

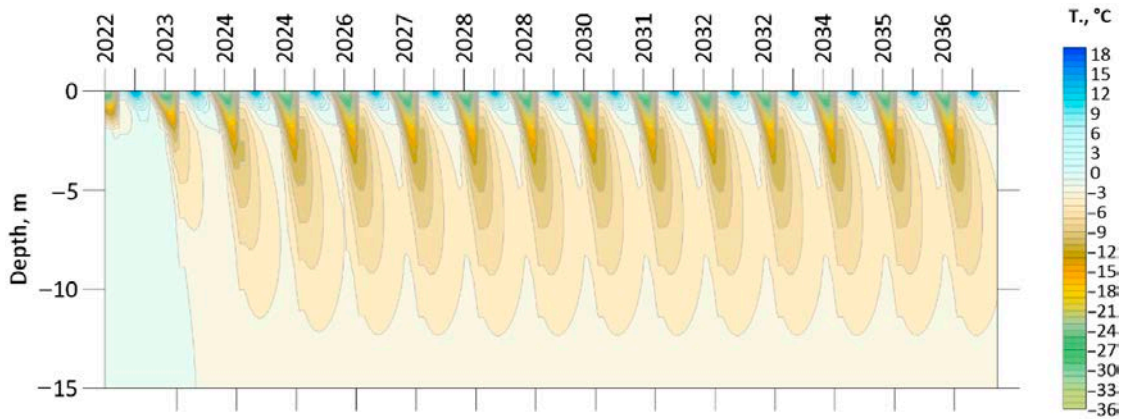
Snow cover was included in the simulations (see Table 3), except for the no-snow scenarios. Snow compaction was only considered in December, January, and February, with the snow depth twice lower and the snow density twice higher. Vegetation was represented in all simulations as surface shading during the warm season [51]. The simulations were run for a 15-year period from 2021 to 2036.

Figure 5 shows the modeled thaw depths for borehole 6 (see Figure 4). As is seen, variant 1 (full saturation) will result in the formation of a thick protective layer (Figure 5a). In variant 2, the protective layer is, on average, 40 cm thinner than in variant 1 (Figure 5b). In variant 3, the thickness of the protective layer is evidently dependent on soil moisture variations, other conditions being equal. It is close to the variant 2 thickness for the periods with natural moisture contents and reaches the variant 1 values when the soils are at full saturation (Figure 5c). In all variants, the protective layer is thickest under snow scenarios II and III, and thinnest under scenario I. Additionally, for comparison, Figure 5 shows the depth curves of the active layer, designated as “ICE”, without any changes in external influences. This scenario is the control for all other scenarios. It was also used to parameterize and analyze the sensitivity of the model.

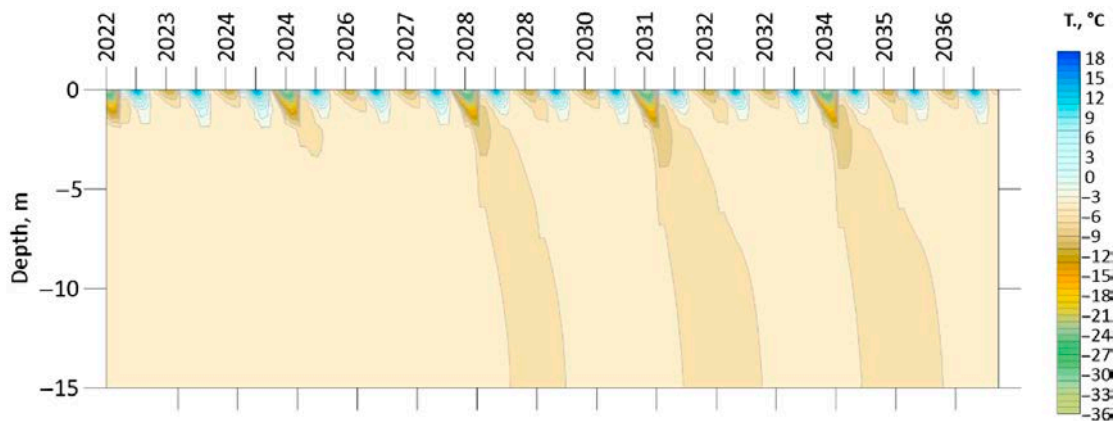


**Figure 5.** The simulated changes in thaw depth for three moisture variants with different snow scenarios. (a)—variant 1; (b)—variant 2; and (c)—variant 3.

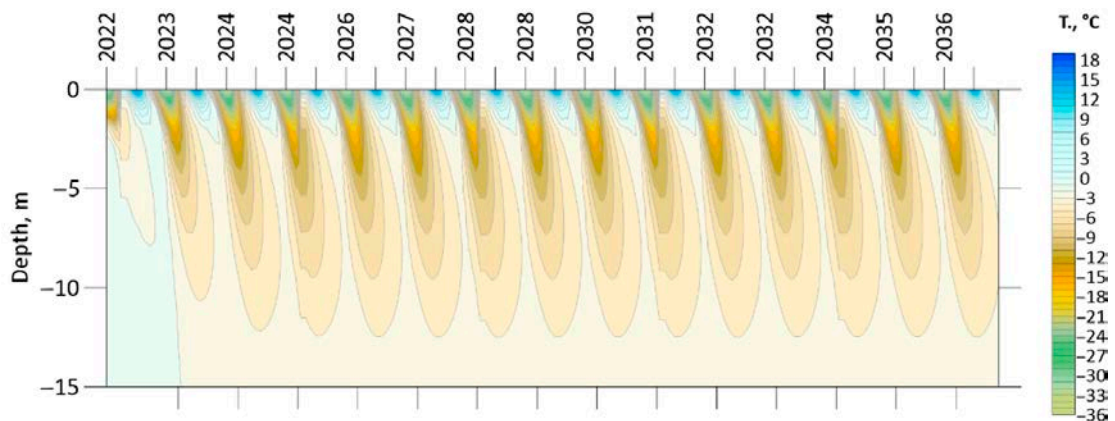
The calculated results of the dynamics of the mean annual temperature of permafrost within the layer of annual temperature variations under the considered variants and scenarios are very diverse and can change, in some cases, over the entire depth (Figure 6). Changes in the mean annual ground temperature will depend on snow conditions. Snow removal throughout the simulation period (scenario II) will result in strong permafrost cooling in all variants, while snow compaction every three years will lead to permafrost temperatures at a 10 m depth in the range from  $-1.2$  to  $2.1$  °C.



(a) Variant: 1-II.

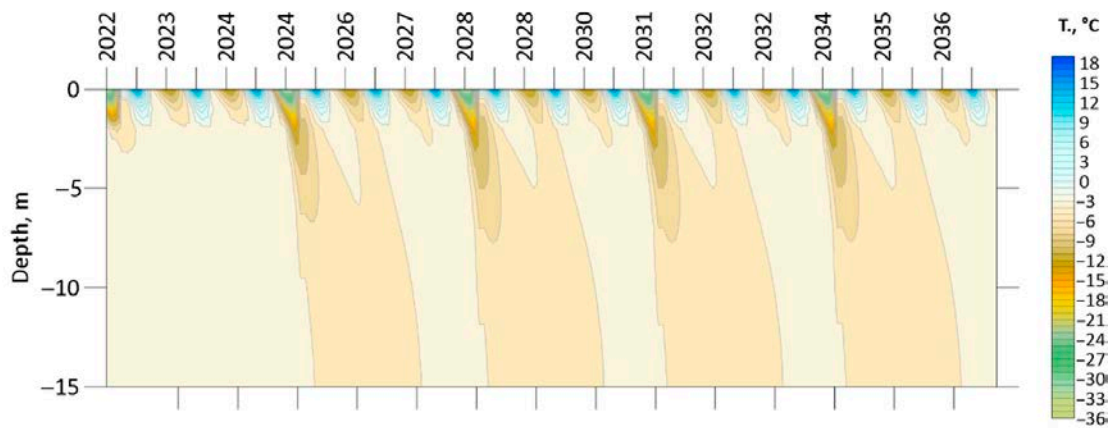


(b) Variant: 1-IV.

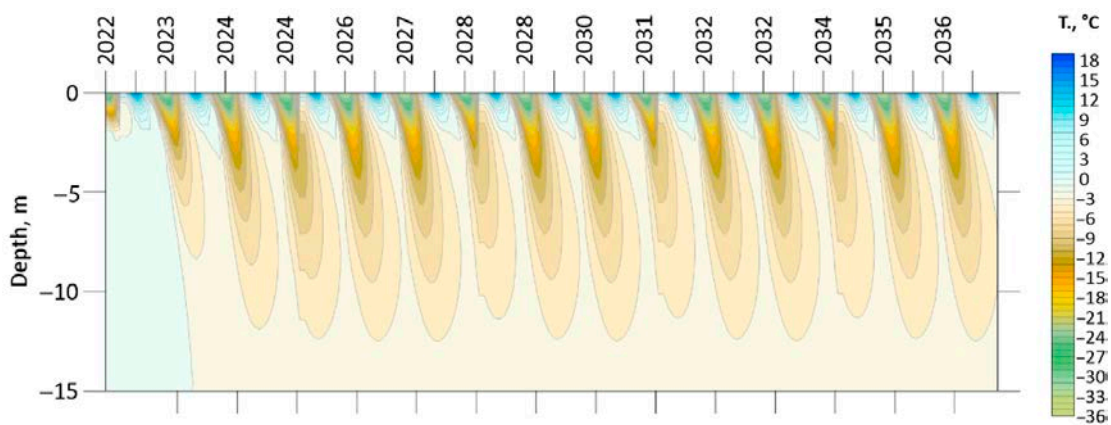


(c) Variant: 2-II.

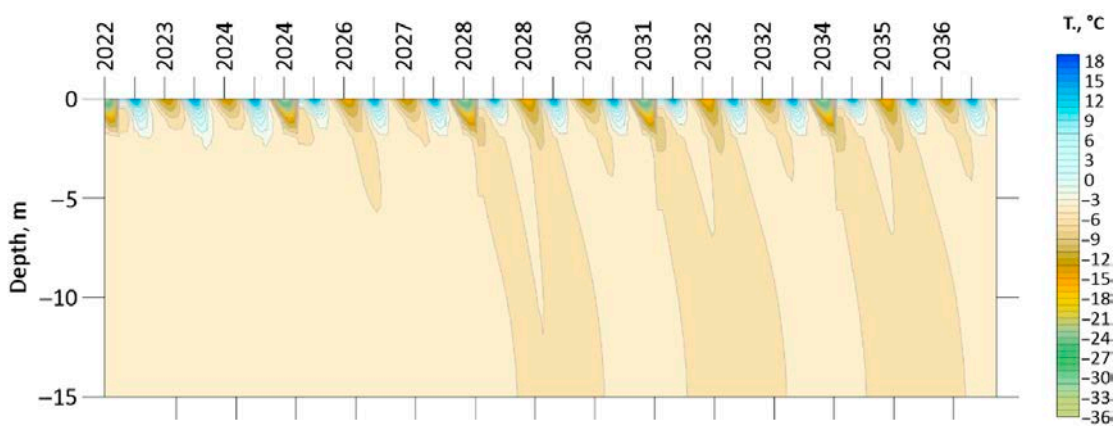
Figure 6. Cont.



(d) Variant: 2-IV.



(e) Variant: 3-II.



(f) Variant: 3-IV.

**Figure 6.** Mean annual dynamics permafrost temperature in 2022 and 2036 under the considered variants and scenarios.

#### 4. Discussion

To analyze the simulation results, a table was compiled showing the optimal conditions for restoring the protective layer (Table 8). The criteria for compiling the table were the conditions for the formation or non-formation of a protective layer for the period under consideration.

**Table 8.** Optimal conditions for protective layer restoration.

Scenario\Variant	1. Saturated Moisture Content	2. Natural Moisture Content	3 Changing Moisture Content
I Snow is absent within the first year and equal to the recent 10-year average in subsequent years			
II Snow removal			
III Snow compaction			
IV Snow compaction every 3 years			
V Snow is absent for the first 3 years and equal to the recent 10-year average in subsequent years			

Red—poor conditions; Yellow—moderate conditions; and Green—good conditions.

The analysis suggests that based on variant 2 (natural moisture content), the thickness of the protective layer will be 40 cm less deep than in variant 1. This is due to the lower water content and, subsequently, ice content of the soil. The lower the ice content, the lower the effective heat capacity of the protective layer and the greater the depth of seasonal thaw. Based on this, the best conditions for restoring the protective layer are achieved in variant 1, which is when the soil moisture contents within the active layer in the warm season are taken to equal the saturated moisture contents (full saturation). This case would lead to a thick ice-enriched layer with the best results under scenarios II and III, when the snow cover is absent or compacted. The optimal restoring under this option, taking into account financial and labor costs, is observed under scenario IV (snow compaction every 3 years).

The advantage of option 1 over option 2 in the formation of a protective layer can be observed in scenarios 1 and 5. Under these scenarios, the protective layer in option 1 lasts 7 years longer than in option 2. This proves that with full moisture capacity (option 1), a thicker and higher heat capacity protective layer is formed.

Variant 3 was applied to find the most optimal option for protective layer restoration. This variant was used for the purpose of economic feasibility of applying the proposed methods for restoring the destroyed territories. Thus, as a result of the analysis of the selection of different combinations, the optimal restoring is observed under scenario IV. In this case, effective protection and preservation of permafrost conditions are observed, which is also confirmed by the dynamics of the temperature regime of soil (see Figure 5).

In all three soil moisture variants, the thickest stable protective layer is achieved after 3 years and varies from 0.3 m to 1.3 m, depending on the active layer moisture conditions. This is explained by the warm conditions in upper permafrost in degrading landscapes [52]. For the specified changes in surface conditions and the initial permafrost temperature profile, the thermal balance would reach a steady state in 3 to 4 years. This is evidenced by the ground temperature dynamics (Figure 7).

It follows that for a thick, ice-enriched layer to develop, soil moisture contents should be increased before the cold season in order to provide a higher effective heat capacity for the active layer. This would promote thinning of the active layer as more heat input is used for phase transitions [35].

In the study area, snow cover is the most important environmental variable influencing permafrost conditions. Monitoring investigations of the surface energy balance conducted earlier in Central Yakutia [50] showed that the insulating effect of snow cover in this area is significantly higher than elsewhere. Thermal conductivity is an important characteristic of the snow cover which is a function of snow density. As snow density increases, its thermal conductivity increases, and hence its insulating effect decreases. Snow removal and snow compaction by artificial or natural means could potentially be used to control permafrost

conditions in a warming climate. This concept underpins the permafrost protection method proposed by Zimov [53,54]. While we generally agree with this approach, we think that frequent and strong cooling of the soils could lead to a replacement of forest vegetation by grassland. This will trigger changes in permafrost conditions and hence modify the entire ecosystem of northern regions.

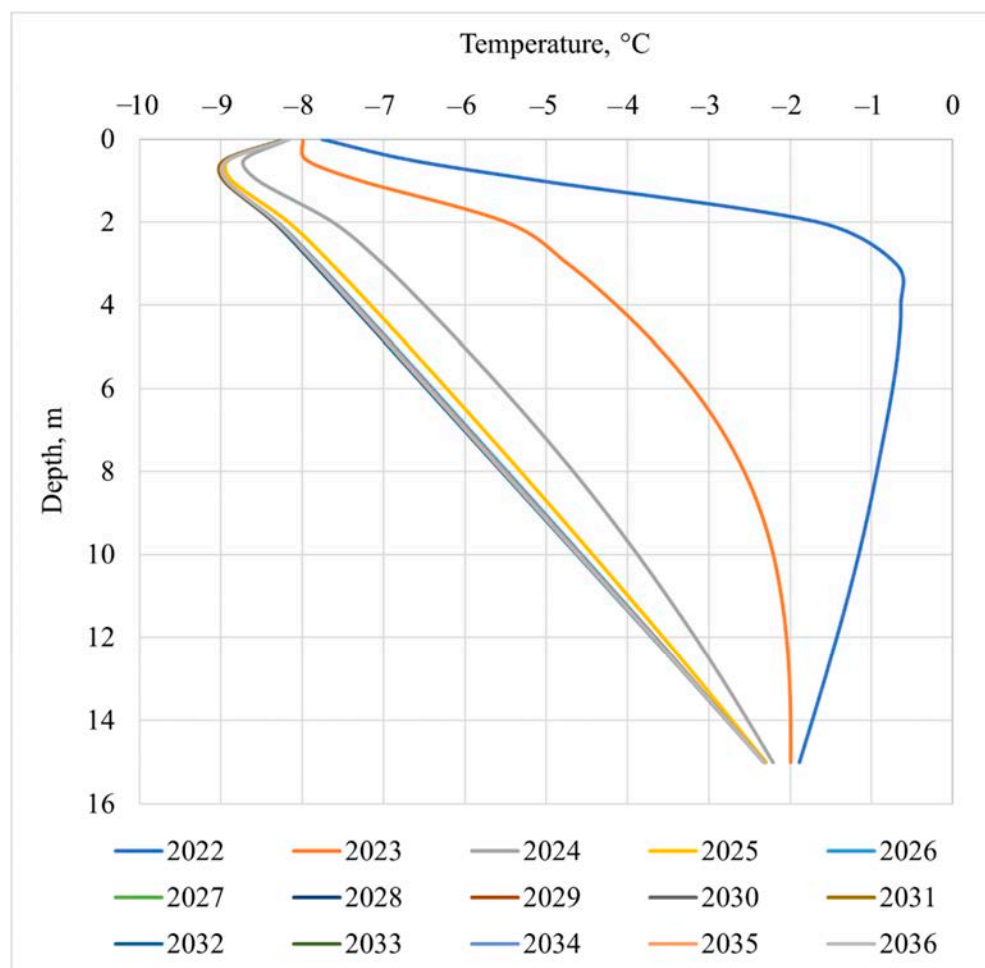


**Figure 7.** Dynamics of mean annual ground temperatures from 2022 to 2036 for variant 1 and scenario II.

Observational data indicate that the temperature regime of permafrost in the boreal forests remains resilient to the current warming of the climate [55], attesting to the insulating role of forest vegetation. Further, permafrost in forested areas has been reported to contain a thick transition layer [11], which serves as a high heat capacity buffer that prevents deep thawing and heat penetration. These data, as well as our study, imply that achieving the stability of permafrost conditions would require a combination of insulating (forest vegetation) and high heat capacity (transition layer) layers in the atmosphere–ground system.

Differences between the previously discovered heating effect of precipitation on permafrost [16,17,20] and our modeled results can be explained by the scale of observation areas, respectively, by different amounts of incoming moisture. In our theoretical experiment, soil moisture was localized in a limited area compared to the area of natural precipitation. In our case, the water that has penetrated through the active layer freezes completely due to the surrounding and underlying permafrost, winter cooling due to snow removal, and subsequent shading due to vegetation restoration. This process leads to the formation of an ice-saturated layer, which thaws more slowly, reducing the thickness of the active layer. At the same time, convective heat transfer due to humidification was small and did not significantly affect the overall heat balance, so a cooling effect is observed.

The heating effect of liquid precipitation on permafrost during an artificial or natural increase in precipitation during the summer season [16,17,20], in most cases, depends on altitude heat-insulating snow cover or a nearby mass of water (lake), which acts as a heat accumulator. As a rule, areas with a cold climate are very dry. For this reason, summer precipitation has practically no effect on the thermal and moisture regime of soils, evaporating almost completely from the surface, provided that they are not abnormally large. Therefore, the depth of thawing of the next year is determined by autumn, pre-winter liquid precipitation. If the moisture coming from the atmosphere completely freezes and cools, then next summer the thawing depth will decrease. Of course, this process is contributed by the snow that fell after autumn, in the winter. If the snow depth is high, then there is not enough cold coming in to freeze and cool the moistened soils. With a small amount of snow in the winter or with relatively late snow accumulation, moistened soils freeze and cool. From this, it follows that, in the general case, the moistening of soil, other things being equal, leads to a warming effect on the thermal regime of soil. However, soil moistening in limited, local areas, with little snow and subject to remoteness from water bodies, can reduce the soil temperature, reducing the thickness of the active layer and recreating an ice-saturated transition layer. This may explain the stability of permafrost conditions observed in some areas despite the increase in mean annual air temperature.

While the forested permafrost landscapes begin to stabilize and recover in five or six years after disturbance [52], thaw-induced changes to the ice-rich anthropogenic landscapes (rural communities, agricultural lands, etc.), lead to intensive degradational processes and land damage. Further activities and land use in such areas will be impossible without protection and mitigation measures, including those presented here.

It is important to note that the proposed method is one of the ways to reduce the depth of the active layer and, consequently, by preventing the thawing of permafrost and the carbon emissions from permafrost.

The next step beyond this modeling study will involve field experimentation to develop techniques for restoring the protective transition layer in the thermokarst-affected areas of Central Yakutia.

## 5. Conclusions

Thermal simulations were carried out for three soil moisture variants and five snow scenarios. An observed ground profile with measured soil physical properties was considered to account for the phase change of the soil moisture. The simulation period was 15 years.

Based on the results and their analysis, the following conclusions are made:

1. The simulation results show that restoration of a protective transition layer for land remediation in thermokarst-affected areas of Central Yakutia is technically feasible.
2. The results suggest that a reliable protective layer will be obtained if the soils are at full saturation before the winter and snow is removed or compacted during the winter. This option will be adopted further in a field experiment.
3. In all three variants, the transition layer reaches its maximum thickness and stability in three years and varies from 0.3 to 1.3 m, depending on the moisture content conditions of the active layer.
4. A combination of heat insulating and high heat capacity layers in the atmosphere–ground system will be necessary to achieve the stability of permafrost conditions.
5. The proposed method is one of the real ways to reduce carbon emissions from permafrost, by preventing the thawing of permafrost.

**Author Contributions:** Conceptualization, A.Z.; methodology, A.Z. and A.K.; software, M.S.; validation, A.Z., M.S. and V.L.; formal analysis, A.K. and Z.W.; investigation, A.Z.; resources, A.Z. and Z.W.; data curation, A.Z. and V.L.; writing—original draft preparation, A.Z. and A.S.; writing—review and editing, A.Z. and A.S.; visualization, M.S. and V.L.; supervision, A.Z.; project administration, A.Z.; funding acquisition, A.Z. and Z.W. All authors have read and agreed to the published version of the manuscript.

**Funding:** This study was funded by the Russian Foundation for Basic Research (grant No. 21-55-15013), the Russian Science Foundation (grant No. 19-78-10088), the Chinese Academy of Sciences President’s International Fellowship Initiative (grant No. 2022VEB003), and the Melnikov Permafrost Institute (project AAAA-A20-120111690010-2).

**Institutional Review Board Statement:** Not applicable.

**Conflicts of Interest:** The authors declare no conflict of interest.

## References

- Shukla, P.; Skea, J.; Slade, R.; van Diemen, R.; Haughey, E.; Malley, J.; Pathak, M.; Pereira, J.P. Technical Summary. In *Climate Change and Land: An IPCC Special Report on Climate Change, Desertification, Land Degradation, Sustainable Land Management, Food Security, and Greenhouse Gas Fluxes in Terrestrial Ecosystems*; Shukla, P., Skea, J., Buendia, E.C., Masson-Delmotte, V., Pörtner, H.-O., Roberts, D.C., Zhai, P., Slade, R., Connors, S., van Diemen, R., et al., Eds.; Cambridge University Press: Cambridge, UK, 2019, *in press*.
- Osterkamp, T.E. The Recent Warming of Permafrost in Alaska. *Glob. Planet. Chang.* **2005**, *49*, 187–202. [[CrossRef](#)]
- Jorgenson, M.T.; Shur, Y.L.; Pullman, E.R. Abrupt increase in permafrost degradation in Arctic Alaska. *Geophys. Res. Lett.* **2006**, *33*, L02503. [[CrossRef](#)]
- Trevor, C.L.; Kokelj, S.V. Increasing Rates of Retrogressive Thaw Slump Activity in the Mackenzie Delta Region, N.W.T., Canada. *Geophys. Res. Lett.* **2008**, *35*. [[CrossRef](#)]
- Hjort, J.; Streletskiy, D.; Doré, G.; Wu, Q.; Bjella, K.; Luoto, M. Impacts of permafrost degradation on infrastructure. *Nat. Rev. Earth Environ.* **2022**, *3*, 24–38. [[CrossRef](#)]
- Streletskiy, A.O.; Suter, L.J.; Shiklomanov, N.I.; Porfirie, B.N.; Eliseev, D.O. Assessment of climate change impacts on buildings, structures and infrastructure in the Russian regions on permafrost. *Environ. Res. Lett.* **2019**, *14*, 025003. [[CrossRef](#)]
- Saito, H.; Iijima, Y.; Basharin, N.I.; Fedorov, A.N.; Kunitsky, V.V. Thermokarst Development Detected from High-Definition Topographic Data in Central Yakutia. *Remote Sens.* **2018**, *10*, 1579. [[CrossRef](#)]
- Lytkin, V.; Suleymanov, A.; Vinokurova, L.; Grigorev, S.; Golomareva, V.; Fedorov, S.; Kuzmina, A.; Syromyatnikov, I. Influence of Permafrost Landscapes Degradation on Livelihoods of Sakha Republic (Yakutia) Rural Communities. *Land* **2021**, *10*, 101. [[CrossRef](#)]
- Available online: <https://tass.ru/interviews/12509211> (accessed on 15 July 2022).
- Fedorov, A.N.; Iwahana, G.; Konstantinov, P.Y.; Machimura, T.; Argunov, R.N.; Efremov, P.V.; Lopez, L.M.C.; Takakai, F. Variability of permafrost and landscape conditions following clear cutting of larch forest in Central Yakutia. *Permafr. Periglac. Process.* **2017**, *28*, 331–338. [[CrossRef](#)]
- Fedorov, A.N.; Konstantinov, P.Y.; Vasilyev, N.F.; Shestakova, A.A. The influence of boreal forest dynamics on the current state of permafrost in Central Yakutia. *Polar Sci.* **2019**, *22*, 100483. [[CrossRef](#)]
- Efimov, A.I.; Grave, N.A. Buried ice in the Abalakh lake area. *Social. Stroit.* **1940**, *1*, 67–78. (In Russian)
- Shur, Y.; Hinkel, K.M.; Nelson, F.E. The transient layer: Implications for geocryology and climate-change science. *Permafr. Periglac. Process.* **2005**, *16*, 5–17. [[CrossRef](#)]
- Yanovsky, V.K. Expedition to Pechora River to determine the position of the southern permafrost boundary. *Rep. Comm. Permafr. Investig.* **1933**, *5*, 65–149. (In Russian)
- Grosse, G.; Romanovsky, V.; Jorgenson, T.; Anthony, K.W.; Brown, J.; Overduin, P.P. Vulnerability and feedbacks of permafrost to climate change. *Eos Trans. Am. Geophys. Union* **2011**, *92*, 73–74. [[CrossRef](#)]
- Magnússon, R.Í.; Hamm, A.; Karsanaev, S.V.; Limpens, J.; Kleijn, D.; Frampton, A.; Maximov, T.C.; Heijmans, M.M. Extremely wet summer events enhance permafrost thaw for multiple years in Siberian tundra. *Nat. Commun.* **2022**, *13*, 1556. [[CrossRef](#)] [[PubMed](#)]
- Douglas, T.A.; Turetsky, M.R.; Koven, C.D. Increased rainfall stimulates permafrost thaw across a variety of Interior Alaskan boreal ecosystems. *NPJ Clim. Atmos. Sci.* **2020**, *3*, 28. [[CrossRef](#)]
- Payette, S.; Delwaide, A.; Caccianiga, M.; Beauchemin, M. Accelerated thawing of subarctic peatland permafrost over the last 50 years. *Geophys. Res. Lett.* **2014**, *31*, 18. [[CrossRef](#)]
- Åkerman, H.J.; Johansson, M. Thawing permafrost and thicker active layers in sub-arctic Sweden. *Permafr. Periglac. Proc.* **2008**, *19*, 279–292. [[CrossRef](#)]
- Iijima, Y.; Fedorov, A.N.; Park, H.; Suzuki, K.; Yabuki, H.; Maximov, T.C.; Ohata, T. Abrupt increases in soil temperatures following increased precipitation in a permafrost region, central Lena River basin, Russia. *Permafr. Periglac. Proc.* **2010**, *21*, 30–41. [[CrossRef](#)]
- Gavriliev, P.P.; Mandarov, A.A. *Basin Irrigation of Meadows in Central Yakutia*; Nauka: Novosibirsk, Russia, 1976; 165p. (In Russian)
- Gavriliev, P.P.; Mandarov, A.A.; Ugarov, I.S. *Hydrothermal Reclamation of Agricultural Lands in Yakutia*; Nauka: Novosibirsk, Russia, 1984; 201p. (In Russian)
- Ugarov, I.S.; Rysakov, Z.I. Soil Moisture Regime in Central Yakutia under Sprinkler Irrigation. In *Permafrost Investigations in Development Areas of the USSR*; Nauka: Novosibirsk, Russia, 1980; pp. 53–57. (In Russian)
- Gavriliev, P.P. Thaw Settlement and Surface Deformation of Reclaimed Fields in the Amga River Valley. In *Cryohydrogeological Investigations*; Permafrost Institute: Yakutsk, Russia, 1985; pp. 148–161. (In Russian)
- Gavriliev, P.P. Special Features of the Irrigation Technology Considering Drought Stress and Permafrost in Yakutia. In *Abstracts of the Regional Conference on Prevention of Adverse Consequences of Soil Irrigation in Siberia*; Nauka: Abakan, Russia, 1988; pp. 21–23. (In Russian)
- Gavriliev, P.P. *Reclamation of Permafrost Lands in Yakutia*; Nauka: Novosibirsk, Russia, 1991; 184p. (In Russian)

27. Gavriliev, P.P. Cryogenic Processes and Variability of Active Layer Parameters in the Ice Complex of Central Yakutia. In Proceedings of the Third International Scientific Conference on the Global Energy and Water Cycle, Beijing, China, 16–19 June 1999; Nagoya University: Nagoya, Japan, 1999; p. 331, EDN VVQZQF.
28. Ugarov, I.S. Microclimate of Sprinkling Irrigation in Central Yakutia on the Example of the Valley of the River Amga. In *Issues of Yakutia Geography*; Yakutsk Scientific Center of the Siberian Branch of the Russian Academy of Sciences: Yakutsk, Russia, 1993; pp. 38–41. (In Russian)
29. Ugarov, I.S. Hydrothermal regime of soils during agricultural development in Central Yakutia. *Cand. Geogr. Sci. Diss. Abstr. Yakutsk* **2001**, 23. (In Russian)
30. Gavriliev, P.P.; Ugarov, I.S.; Efremov, P.V. *Permafrost-Ecological Characteristics of Taiga Agrolandscapes, Central Yakutia*; Permafrost Institute SB RAS: Yakutsk, Russia, 2001; 196p. (In Russian)
31. Ugarov, I.S. Experience in restoring disturbed agricultural lands. *Adv. Curr. Nat. Sci.* **2012**, 11 Pt 1, 137–139. (In Russian)
32. Wen, Z.; Niu, F.; Yu, Q.; Wang, D.; Feng, W. The role of rainfall in the thermal-moisture dynamics of the active layer at Beiluhe of Qinghai-Tibetan plateau. *Environ. Earth Sci.* **2014**, 71, 1195–1204. [[CrossRef](#)]
33. Zhang, M.; Wen, Z.; Li, D.; Chou, Y.; Zhou, Z.; Zhou, F.; Lei, B. Impact process and mechanism of summertime rainfall on thermal moisture regime of active layer in permafrost regions of central Qinghai Tibet Plateau. *Sci. Total Environ.* **2021**, 796, 148970. [[CrossRef](#)]
34. Zhirkov, A.F.; Zhelezniak, M.N.; Permyakov, P.P.; Kirillin, A.R.; Verkhoturov, A.G. Influence of rainfall infiltration on the thermal regime of frozen soils. *Vestn. Trans Baikal Univ.* **2018**, 24, 4–14. (In Russian) [[CrossRef](#)]
35. Zhirkov, A.; Permyakov, P.; Wen, Z.; Kirillin, A. Influence of rainfall changes on the temperature regime of permafrost in Central Yakutia. *Land* **2021**, 10, 1230. [[CrossRef](#)]
36. Zhirkov, A.F.; Wen, Z.; Permyakov, P.P.; Zhelezniak, M.N.; Gao, Q.; Kirillin, A.R. Numerical simulation of the subsoil condensation process and its impact on the heat and moisture regime of the frozen soils. *Int. J. Adv. Biotechnol. Res.* **2019**, 10, 372–386.
37. Smirnov, N.S. *Scientific and Applied Reference Book on the Climate of the USSR*; Series 3; Long-Term Data Parts 1–6; Book 1; Gidrometeoizdat: Leningrad, Russia, 1989; p. 607. (In Russian)
38. Zhelezniak, M.N. *Permafrost-Landscape Map of the Republic of Sakha (Yakutia), Scale 1:1,500,000*; Melnikov Permafrost Institute SB RAS: Yakutsk, Russia, 2018.
39. No. POCC RU.HB61.H25485; Frost 3D Software Package. Certificate of Compliance; Engineering Software Certification Center: Moscow, Russia, 2021.
40. Samarsky, A.A.; Gulin, A.V. *Numerical Methods in Mathematical Physics*; Nauchny Mir: Moscow, Russia, 2003; 316p. (In Russian)
41. Kurtner, D.A.; Chudnovsky, A.F. *Calculation and Control of the Thermal Regime in Open and Covered Soil*; Gidrometeoizdat: Leningrad, Russia, 1969. (In Russian)
42. Leontev, N.E. *Fundamentals of Fluid Flow Theory*; MSU Faculty of Mechanics and Mathematics: Moscow, Russia, 2009; 88p. (In Russian)
43. Samarsky, A.A. *Theory of Finite Difference Schemes*, 3rd ed.; Nauka: Moscow, Russia, 1989; 616p. (In Russian)
44. Available online: <https://rp5.ru/> (accessed on 1 May 2022).
45. Air Temperature. In *USSR Climate Data Handbook*; Gidrometeoizdat: Leningrad, Russia, 1989; Volume 24, Part 1; p. 545.
46. *Republican Building Code 87-67*; Engineering Site Investigations; Prediction of Permafrost Temperature Regime Changes by Numerical Methods: Moscow, Russia, 2003. (In Russian)
47. Gorelik, J.B.; Pazderin, D.S. Correctness of formulation and solution of thermotechnical problems in forecasting temperature field dynamics in the foundations of constructions on permafrost. *Kriosf. Zemli* **2017**, 21, 49–59.
48. Skachkov, Y.B. Review of Recent Climatic and Environmental Changes in the Republic of Sakha (Yakutia). In *Review of Recent Climatic and Environmental Changes in the Republic of Sakha (Yakutia)*; YSU: Yakutsk, Russia, 2010; pp. 1–6. (In Russian)
49. Skachkov, Y.B. Climate change trends in Central Yakutia at the turn of the XX–XXI centuries. In Proceedings of the International Conference Regional Environmental Response to Global Changes in Northeastern and Central Asia, Irkutsk, Russia, 17 September 2012; pp. 236–238. (In Russian).
50. Pavlov, A.V. *Heat Exchange between the Soil and Atmosphere in Northern and Temperate Latitudes of the USSR*; Yakutsk Publ. House: Yakutsk, Russia, 1975; 302p. (In Russian)
51. Permyakov, P.P.; Zhirkov, A.F.; Varlamov, S.P.; Skryabin, P.N.; Popov, G.G. Numerical Modeling of Railway Embankment Deformations in Permafrost Regions, Central Yakutia. In *Transportation Soil Engineering in Cold Regions*; Petriaev, A., Konon, A., Eds.; Lecture Notes in Civil Engineering; Springer: Singapore, 2020; Volume 2. [[CrossRef](#)]
52. Fedorov, A.N.; Konstantinov, P.Y. Response of permafrost landscapes of Central Yakutia to current changes of climate, and anthropogenic impacts. *Geogr. Nat. Resour.* **2009**, 30, 146–150. [[CrossRef](#)]
53. Zimov, S.A. Pleistocene Park: Return of the mammoth’s ecosystem. *Science* **2005**, 308, 796–798. [[CrossRef](#)]
54. Beer, C.; Zimov, N.; Olofsson, J.; Porada, P.; Zimov, S. Protection of permafrost soils from thawing by increasing herbivore density. *Sci. Rep.* **2020**, 10, 4170. [[CrossRef](#)]
55. Varlamov, S.P.; Skachkov, Y.B.; Skryabin, P.N. Influence of climate change on the thermal condition of Yakutia’s permafrost landscapes (Chabyda Station). *Land* **2020**, 9, 132. [[CrossRef](#)]

**Disclaimer/Publisher’s Note:** The statements, opinions and data contained in all publications are solely those of the individual author(s) and contributor(s) and not of MDPI and/or the editor(s). MDPI and/or the editor(s) disclaim responsibility for any injury to people or property resulting from any ideas, methods, instructions or products referred to in the content.